Dalton Transactions

PAPER

View Article Online
View Journal | View Issue

Check for updates

Cite this: *Dalton Trans.*, 2023, **52**, 3052

Imine-stabilized silylium ions: synthesis, structure and application in catalysis†

Aymeric Dajnak,[a] Limiao Shi,[a] Gül Altınbaş Özpınar,[b] Romaric Lenk,[a] Nathalie Saffon-Merceron,[c] Antoine Baceiredo,[a] Tsuyoshi Kato,[a] Thomas Müller[b] and Eddy Maerten *[a]

Received 18th January 2023,
Accepted 3rd February 2023

DOI: 10.1039/d3dt00168g

rsc.li/dalton

Novel norbornene-based imine-stabilized silylium ions **2** have been synthesized *via* the simple reaction of sulfide-stabilized silylium ion **1** with carbonyl derivatives. Those silylium ions were fully characterized in solution and in the solid state by NMR spectroscopy and X-ray diffraction analysis as well as DFT calculations. Unlike the previously reported phosphine-stabilized silylium ion **VI**, behaving as a Lewis pair, calculations show that **2** have a strong Lewis acid character. Indeed, imine-stabilized silylium ions **2** are able to activate Si–H bonds and catalyzed the hydrosilylation of carbonyl derivatives under mild conditions.

Introduction

Since the isolation of the first stable free silylium ion **I** (Fig. 1) by Reed and Lambert in 2002,[1] considerable effort has been devoted to studying the chemistry of silylium ions.[2] The accumulation of knowledge has allowed the development of stabilized systems that are easy to handle while preserving their unique reactivity and exceptional Lewis acidity. Of particular interest, the use of a weak Lewis base on the cationic silicon atom **II** has proven to be an excellent methodology[3] to find a good compromise between stability and reactivity, making those species useful as synthetic tools that can be applied in various transformations.[4] One of the best examples is the ferrocenium-stabilized silylium ion **III**, developed by Oestreich's group.[5] Indeed, this species is by far the most efficient catalyst to promote the Diels–Alder reaction in good yields at low temperature so far, even with challenging dienophile/diene combinations.[6] Interestingly, silylium ion **III** also smoothly catalyze in mild conditions the hydrosilylation reaction of carbonyl derivatives.[7] Another particularity of silylium ions lies in their potential to activate C–F bonds, due to the strong affinity between silicon and fluoride. Thus, catalysts of type **IV** and **V** are together with Ozerov's trialkylsilylium-carborane systems efficient catalysts for hydrodefluorination reactions.[8,9] Obviously, the stability/reactivity balance of these species is strongly related to the choice of Lewis base ligand, which is crucial for their catalytic activity.

We recently reported the synthesis of phosphine- and sulfide-stabilized silylium ions **VI** and **1** with a particular norbornene-based framework connecting the silylium ion and the donor ligand (Fig. 1 and Scheme 1).[10] Interestingly, we have

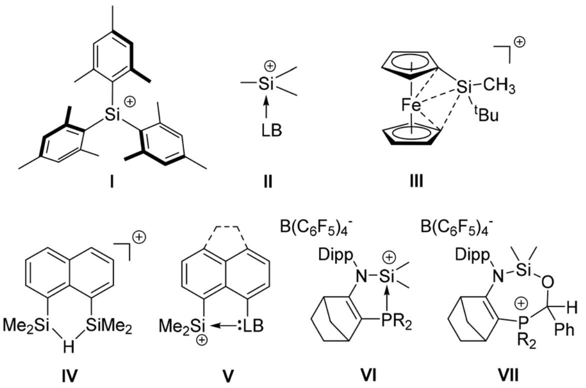

Fig. 1 Free silylium ion **I** and Lewis base-stabilized silylium ions **II–VII**.

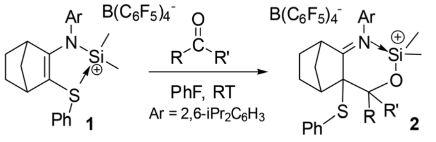

	R	R'
a	H	Ph
b	CH_3	Ph
c	CF_3	Ph
d	Et	Et
e	Ph	Ph

Scheme 1 Synthesis of sulfide-stabilized silylium ions **2**.

---

[a] *Université de Toulouse, UPS, and CNRS, LHFA UMR 5069, 118 route de Narbonne, 31062 Toulouse, France. E-mail: eddy.maerten@univ-tlse3.fr*

[b] *Institute of Chemistry, Carl von Ossietzky University, Oldenburg, D-26129 Oldenburg, Germany*

[c] *Université de Toulouse, UPS, and CNRS, ICT UAR2599, 118 route de Narbonne, 31062 Toulouse, France*

† Electronic supplementary information (ESI) available. CCDC 2234864. For ESI and crystallographic data in CIF or other electronic format see DOI: **https://doi.org/10.1039/d3dt00168g**

demonstrated that these two silylium ions exhibit very different reactivity toward methyl acrylate. Indeed, due to the moderate flexibility of the ligand framework and its strong nucleophilic character, despite its high stability, phosphine-stabilized silylium ions **VI** behave as a Lewis pair and undergo ambiphilic type reactions leading to nine-membered heterocycles.[10a] Similarly, **VI** reacts with benzaldehyde to give the carbonyl insertion product **VII**. In contrast, the sulfide-stabilized silylium ion **1** acts as a simple Lewis acid due to a less nucleophilic character of sulfide ligand and efficiently catalyzes the Diels–Alder reaction with various olefins.[10b] Here, we report that the sulfide-stabilized silylium ion **1**[11] reacts with various carbonyl derivatives in a peculiar way, polar [4 + 2]-cycloaddition, allowing to synthesize the original imine-stabilized silylium ions **2**, which are efficient catalysts for hydrosilylation and allylsilylation reactions.

Results and discussion

Sulfide-stabilized silylium ion **1** readily reacts with benzaldehyde at room temperature to give the corresponding imine-stabilized silylium ion **2a** (Scheme 1). Cation **2a** was isolated as an air-sensitive yellow-orange powder (isolated yield: 44%). **2a** was obtained as a mixture of two diastereomers (75 : 25) as indicated by the presence of two sets of signals in the NMR spectra in the same ratio. In the ^{29}Si-NMR spectrum, two signals appear at higher field (12.3/7.4 ppm, major/minor products respectively) compared to the sulfide-stabilized silylium ion **1** (54.3 ppm). These chemical shifts are in good agreement with that of previously reported imine-stabilized silylium ions.[11a,12] In the ^{13}C- and the ^{1}H-NMR spectra, the two isomers of **2a** exhibit two sets of singlet signals at 76.9 and 80.4 ppm and at 5.60 and 5.44 ppm, respectively corresponding to the former carbonyl group.

Interestingly, similar reactivity of **1** was observed with different carbonyl compounds affording the corresponding imine-stabilized silylium ions **2b–e** in good yields (Scheme 1). The less nucleophilic trifluoroacetophenone reacts more slowly with **1** This suggests that the reaction starts with carbonyl coordination on the cationic Si atom of **1**. The following nucleophilic attack of enamine on the activated carbonyl carbon center completes the reaction. Indeed, the highly electron-poor perfluoroacetophenone $[(CF_3)(C_6F_5)C{=}O]$ is totally unreactive. All the ^{29}Si NMR signals of the different base-stabilized silylium ions **2a–e** appear in the area of 5.5–12.3 ppm. In ^{13}C NMR spectra, the chemical shift of Si-coordinated imine fragment can be found between 210.5 and 213.2 ppm, which is the typical region for iminium carbon atoms (or Lewis acid coordinated imines).[11a,12]

The structure of **2e** was unambiguously confirmed by an X-ray diffraction analysis (Fig. 2). Yellow crystals were obtained in good yield (85%) from a saturated chloroform solution. The molecular structure of **2e** exhibits a relatively short C2–N1 bond [1.292(5) Å] and a planar environment (Σ° = 359.7°) characteristic of the imine fragment. The N1–Si1 bond length is significantly elongated [1.839(3) Å] compared to that observed in **1** [1.737(2) Å], in agreement with a $N \rightarrow Si^+$ dative character.

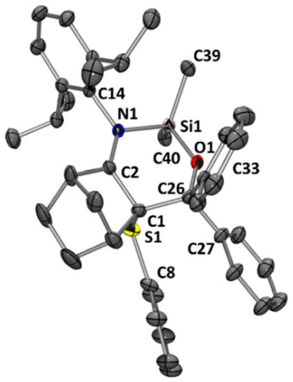

Fig. 2 Molecular structure of cationic part of imine-stabilized silylium borate **2e**. Thermal ellipsoids represent 30% probability. H and disordered atoms, counterion $[B(C_6F_5)_4]^-$ and solvent molecule were omitted for clarity. Selected bond lengths [Å] and angles [°]: N1–Si1 1.839(3), Si1–O1 1.614(3), C26–O1 1.428(5), S1–C1 1.857(4), C1–C2 1.550(6), C2–N1 1.292(5), N1–C14 1.484(5), S1–C8 1.804(4), C26–C33 1.542(6), C26–C27 1.559(9), Si1–C39 1.823(4), Si1–C40 1.838(4); N1–Si1–O1 99.8(1), Si1–O1–C26 135.4(2), C26–C1–C2 111.6(3), C1–C2–N1 124.3(4), C2–N1–Si1 120.0(3), O1–C26–C1 105.8(3), C2–N1–C14 120.9 (3), C14–N1–Si1 118.8(2), O1–Si1–C39 111.8(2), O1–Si1–C40 112.4(2).

To gain more insight into the electronic structure of imine-stabilized silylium ion **2**, DFT calculations have been performed at the M062X/def-2TZVP level of theory. At this level, the optimized molecular structure of **2a**, **2c** and **2e** are very similar and the structure of **2e** is in good agreement with all relevant parameters experimentally observed (see Table S3†). The results of the computations indicated that the formation of cation **2a** is favoured by 80 kJ mol^{-1} over the FLP-type carbonyl insertion product into the S–Si bond of silylium ion **1** (similar to the carbonyl insertion product **VII**, see also Table S2†).

The electrophilic center of cations **2** is the imine carbon atom. Similarly to the case of imine-stabilized silylium ions described by Inoue,[12a] the LUMO corresponds in all cases to the π* orbital of the C=N double bond (see Fig. 3 and Fig. S30†). In addition, the electrostatic potential map of cation **2a** shows the most positive potential around the imine group (Fig. S31†).

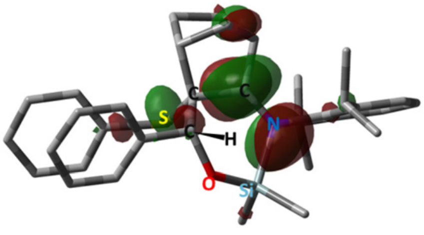

Fig. 3 Optimized molecular structure of cation **2a** and calculated surface diagram of its LUMO (E = −4.24 eV, isodensity value: 0.04).

The electronic structure of cations **2** is similar to those of typical stabilized silyl cations such as **V** and **VI**.[2e,8j,10] Taking into account the steric shielding around the imine group, we suggest that the Lewis acidity of cations **2** arises from reaction of nucleophiles at the silicon center. The Lewis acidity of **2** is high as they are able to activate even Si–H bonds.[13] Indeed, H/D exchange between two deuterated/non-deuterated silanes (Et_3Si-D/$PhMe_2SiH$) in the presence of 10 mol% of **2** was evidenced either at 60 °C or at room temperature (Fig. 4). After 12 h at 60 °C in presence of 10 mol% of **2a**, the reaction attains the equilibrium with a thermodynamic ratio (38 : 62) of Et_3SiD/Et_3SiH (or $PhMe_2SiH/Et_3SiH$). Even with a large excess of silane and a prolongated heating time, NMR data of catalyst **2** remain unchanged. Of particular interest, the equilibrium is achieved at room temperature in less than 2 h with **2c**, which demonstrates that the Lewis acid character of **2** is strongly related to the nature of substituents on the carbon atom next to the oxygen and can be easily modulated just by changing the carbonyl derivative used.

Silylium ion **2a** also efficiently catalyzes the hydrosilylation and allylsilylation of benzaldehyde with triethylsilane and allyltrimethylsilane respectively. Indeed, in presence of 2 or 10 mol% of **2a** at room temperature, both reactions are quantitative in 15 min (isolated yield: 92% and 99% respectively, Scheme 2). The same results were obtained in the presence of a proton sponge (2,6-di-*tert*-butylpyridine), excluding a Brønsted acid catalysis due to a possible hydrolysis of **2a**.

Then the potential catalytic activity of silylium ions **2** in hydrosilylation of ketones has been evaluated (Table 1). For this purpose, we have started this study with the hydrosilylation of acetophenone in the presence of triethylsilane using different catalysts **2a–e** (10 mol%) in order to evaluate the influence of catalyst substituents. The hydrosilylation in the presence of **2a** (10 mol%) as catalyst at room temperature results in a quasi-full conversion of acetophenone in 4 hours affording two products, the silylated alcohol **A** and ethylbenzene **B** which is the result of the reaction of **A** with a second equivalent of silane, in the proportion of 87 : 10 (Table 1, entry 2). This full deoxygenation reaction is often observed when hydrosilylation is promoted by silylium ions.[14] A prolongated reaction time slowly increases the proportion of **B** (**A** : **B** = 74 : 21 in 29 h, Table 1, entry 3). Catalysts **2a**, **2b**, **2d** and **2e**, respectively with H/Ph, CH_3/Ph, Et/Et and Ph/Ph substituents, present similar catalytic activities, leading to quasi-full conversions (95% to 99%) after 4 h with similar **A** : **B** proportions (75 : 14 to 87 : 10, Table 1, entries 2, 5, 11 and 14).[15] In contrast, in the case of catalyst **2c** with an electron-withdrawing CF_3 substituent, the consumption rate of acetophenone is similar but the reduction of the silylated alcohol is much faster since 51% of **B** is already formed when all acetophenone is consumed in 4 h (Table 1, entry 8). A full deoxygenation takes place in less than 29 h (Table 1, entry 9). Therefore, considering the catalytic activity, we decided then to check the scope of the reaction with different carbonyl substrates using catalyst **2c** with CF_3/Ph substituents (Table 2).

$$Et_3SiD + PhMe_2SiH \xrightleftharpoons{\textbf{2}\ (10\ mol\%)} Et_3SiH + PhMe_2SiD$$

	R	R'	T [°C]	time[a),b)]
2a	H	Ph	60	12 h
2c	CF_3	Ph	rt	1.5 h

Fig. 4 H/D exchange between Et_3SiD and $PhMe_2SiH$ catalyzed by **2**. (a) Time to achieve the 38 : 62 ratio of Et_3SiD/Et_3SiH. (b) Determined by ^1H-NMR monitoring of $PhMe_2SiH/Et_3SiH$.

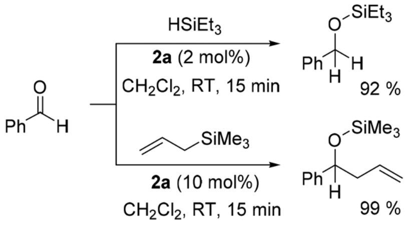

Scheme 2 Hydrosilylation and allylsilylation of benzaldehyde catalyzed by **2a**.

Table 1 Hydrosilylation of acetophenone using triethylsilane catalyzed by imine-stabilized silylium ions **2a–2e**

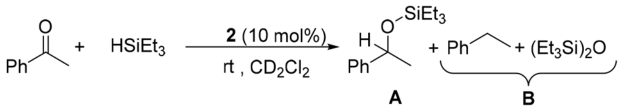

Entry[a]	Catalyst (10 mol%)	R	R′	Time (h)	Conv.[b] (%)	A[c]	B[c]
1	**2a**	H	Ph	2	61	52	4
2				4	97	87	10
3				29	99	74	21
4	**2b**	CH_3	Ph	2	48	40	4
5				4	99	87	10
6				29	99	68	32
7	**2c**	CF_3	Ph	2	76	43	30
8				4	99	43	51
9				29	99	0	99
10	**2d**	Et	Et	2	85	74	7
11				3	95	78	11
12				25	99	67	25
13	**2e**	Ph	Ph	2	52	34	14
14				4	95	75	14
15				23	99	61	28

[a] Reactions were carried out by using 0.25 mmol of acetophenone, triethylsilane (2.1 equiv., 0.53 mmol) and 10 mol% of **2** in 1 mL of CD_2Cl_2 in presence of 0.041 mmol of hexamethylbenzene used as internal standard. [b] Conversions were determined by ^1H NMR analysis following acetophenone consumption compared to hexamethylbenzene (*D*1 = 10 s). [c] Formation of products **A** and/or **B** were determined by ^1H NMR analysis of the crude compared to hexamethylbenzene (*D*1 = 10 s).

In contrast to the case of acetophenone (Table 1, entry 9), hydrosilylation reactions of trifluoroacetophenone and diethylketone using catalyst **2c** (10 mol%, at room temperature) are selective and afford the hydrosilylated alcohol **C** as single product (Table 2, entries 3 and 5). However, despite the clean

Table 2 Hydrosilylation of ketones using triethylsilane with imine-silylium ion **2c**

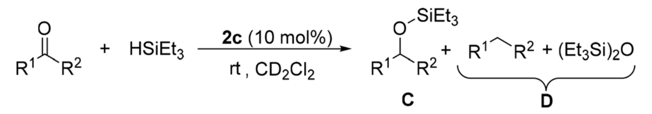

Entry[a]	R^1	R^2	Time (h)	Conv.[b] (%)	C[c]	D[c]
1	Ph	CF_3	2	13	13	0
2			4	67	67	0
3			7	99	99	0
4	Et	Et	2	4	4	0
5			72	43	43	0
6	Ph	Ph	2	99	58	41
7			4	99	0	99

[a] Reactions were carried out by using 0.25 mmol of carbonyl derivative, triethylsilane (2.1 equiv., 0.53 mmol) and 10 mol% of **2c** in 1 mL of CD_2Cl_2 in presence of 0.041 mmol of hexamethylbenzene used as internal standard. [b] Conversions were determined by ^1H NMR analysis following acetophenone consumption compared to hexamethylbenzene (*D*1 = 10 s). [c] Formation of products **C** and/or **D** were determined by ^1H NMR analysis of the crude compared to hexamethylbenzene (*D*1 = 10 s).

and rapid reaction with the trifluoroacetophenone (full conversion in 7 h, Table 2, entry 3) the hydrosilylation of diethylketone is sluggish and leads to low conversion even after prolonged reaction time (43% in 72 h, Table 2, entry 5) probably due to the decomposition of catalyst during the reaction. Contrary to these selective reactions, in the case of more reactive benzophenone, the reaction is not selective any more. Indeed, a full conversion of benzophenone is obtained in 2 h, leading to a 58 : 41 mixture of the corresponding silylated alcohol **C** and **D** (Table 2, entry 6). In 4 h, silylated alcohol **C** is fully converted into diphenylmethane together with hexaethyldisiloxane (Table 2, entry 7).

Conclusions

In conclusion, the imine-stabilized silylium ions **2**, which can be easily obtained by simple reaction between the sulfide-stabilized-silylium ion **1** and carbonyl derivatives, were found to be strong Lewis acids able of activating Si–H bonds and effectively catalyzing the hydrosilylation and allylsilylation of carbonyl derivatives. Because of the simplicity of the synthesis, derivatization of **2** is particularly easy and its Lewis acidity can be tuned just by changing the carbonyl derivative employed. Efforts are currently underway to expand the diversity of catalytic applications of **2**.

Experimental

General procedures

All manipulations were performed under an inert atmosphere of argon by using standard Schlenk techniques or high-pressure NMR tube techniques. Dry and oxygen-free solvents were used. ^1H, ^{11}B, ^{13}C, ^{19}F and ^{29}Si NMR spectra were recorded on Brucker Avance II 300 MHz, Avance III HD 400 MHz and Avance I and II 500 MHz spectrometers. Chemical shifts are expressed in parts per million with residual solvent signals as internal reference (^1H, ^{29}Si and $^{13}C\{^1H\}$). ^{19}F chemical shifts were reported in ppm relative to $CFCl_3$. The following abbreviations and their combinations are used: br, broad; s, singlet; d, doublet; t, triplet; q, quartet; m, multiplet. ^1H and ^{13}C resonance signals were attributed by means of 2D COSY, HSQC and HMBC experiments. The sulfide-stabilized silylium ion **1** was synthesized as previously reported.[10b] All commercially available reagents were used after drying and/or distillation in proper conditions.

Synthesis of 2a. To a solution of **1** (150 mg, 0.13 mmol) in benzene (2.0 mL) was added benzaldehyde (13.7 μL, 0.13 mmol). Reaction mixture was stirred for two hours and two phases were formed, the upper phase was removed and the lower phase washed twice with benzene (0.3 mL). Lower phase was dried under vacuum to obtained the adduct **2a** as a yellow-orange powder (71.6 mg, 44%). M.p. = 74 °C (decomposition).

Major isomer (75%). ^1H NMR (500 MHz, CD_2Cl_2): = 0.48 (s, 3H, Si–CH_3), 1.17 (s, 3H, Si–CH_3), 1.28 (d, $^3J_{H-H}$ = 6.8 Hz, 3H, CH_{3iPr}), 1.31 (d, $^3J_{H-H}$ = 6.6 Hz, 3H, CH_{3iPr}), 1.40 (d, $^3J_{HH}$ = 6.8 Hz, 3H, CH_{3iPr}), 1.42 (d, $^3J_{H-H}$ = 6.6 Hz, 3H, CH_{3iPr}), 1.83–1.65 (m, 1H, CH_2), 2.17–1.86 (m, 3H, 3CH_2), 2.43–2.31 (m, 2H, 2CH_2), 2.47 (sept, $^3J_{H-H}$ = 6.6 Hz, 1H, CH_{iPr}), 2.99–2.85 (sept, 1H, CH_{iPr} overlapped by signals of minor isomer), 3.34–3.27 (m, 2H, 2$CH_{bridgehead}$), 5.60 (s, 1H, CHO), 6.39–6.33 (m, 2H, CH_{PhCHO}), 7.01–6.97 (m, 2H, CH_{PhCHO}), 7.13–7.06 (m, 1H, CH_{PhCHO}), 7.73–7.28 (m, 8H, 5 S(C_6H_5) and 3CH_{dipp}). ^{13}C NMR (126 MHz, CD_2Cl_2): δ = 0.2 (s, Si–CH_3), 3.3 (s, Si–CH_3), 24.5 (s, CH_{3iPr}), 24.7 (s, CH_{3iPr}), 25.4 (s, CH_2), 25.8 (s, CH_{3iPr}), 26.1 (s, CH_{3iPr}), 26.7 (s, CH_2), 28.6 (s, CH_{iPr}), 29.7 (s, CH_{iPr}), 40.6 (s, CH_2), 43.6 (s, $CH_{bridgehead}$), 49.3 (s, $CH_{bridgehead}$), 68.5 (s, C–S), 76.9 (s, CH–O), 124.6 (br, *i* of BAr), 127.2 (s, CH_{dipp}), 127.3 (s, CH_{dipp}), 127.3 (s, CH_{Ph}), 128.2 (s, CH_{Ph}), 128.7 (s, CH_{Ph}), 129.2 (s, CH_{Ph}), 129.8 (s, CH_{Ph}), 130.3 (s, CH_{Ph}), 131.9 (s, C_{Ph}), 132.2 (s, CH_{dipp}), 132.6 (s, N–C_{Dipp}), 135.5 (s, C_{Ph}), 135.5 (s, C_{PhCHO}), 136.6 (br d, J_{C-F} = 244.8 Hz, ArC–F), 138.6 (br d, J_{C-F} = 244.8 Hz, ArC–F), 142.2 (s, C_{iPr}), 143.8 (s, C_{iPr}), 148.5 (br d, J_{C-F} = 241.3 Hz, ArC–F), 212.0 (s, N–C). ^{19}F NMR (471 MHz, CD_2Cl_2): δ = −167.6 (t, J_{FF} = 19.2 Hz, *m* of ArC–F), −163.7 (t, J_{FF} = 20.4 Hz, *p* of ArC–F), −133.1 (br, o of ArC–F). ^{11}B NMR (160 MHz, CD_2Cl_2): δ = −16.7 (s, BAr_4). ^{29}Si NMR (99 MHz, CD_2Cl_2): δ = 12.3 (s, Si–CH_3).

Minor isomer (25%). All signals marked with *are overlapped by signals of the major isomer. ^1H NMR (500 MHz, CD_2Cl_2): δ = 0.62 (s, 3H, Si–CH_3), 1.00 (d, $^3J_{H-H}$ = 6.7 Hz, 3H, CH_{3iPr}), 1.25–1.21 (m, 1H, CH_2*), 1.26 (d, 3H, CH_{3iPr}*), 1.33 (s, 3H, Si–CH_3*), 1.40 (d, 3H, CH_{3iPr}*), 1.48 (d, $^3J_{HH}$ = 6.6 Hz, 3H, CH_{3iPr}), 1.83–1.65 (m, 3H, CH_2*), 2.17–1.86 (m, 2H, CH_2*), 2.66 (sept, $^3J_{H-H}$ = 6.6 Hz, 1H, CH_{iPr}), 2.99–2.85 (m, 4H, 2$CH_{bridgehead}$ + CH_{iPr} + 1H CH_2*), 5.44 (s, 1H, CHO), 7.14–7.06 (m, 1H, CH_{PhCHO}*),7.73–7.28 (m, 12H, all Ar* signal excepted for 1H CH_{PhCHO}). ^{13}C NMR (126 MHz, CD_2Cl_2): δ = 0.8 (s, Si–CH_3), 4.8

(s, Si–CH_3), 24.6 (s, CH_{3iPr}), 24.7 (s, CH_{3iPr}), 24.7 (s, CH_{3iPr}), 25.0 (s, CH_{3iPr}), 25.2 (s, CH_2), 25.9 (s, CH_{3iPr}), 27.6 (s, CH_2), 28.8 (s, CH_{iPr}), 29.1 (s, CH_{iPr}), 38.3 (s, CH_2), 44.8 (s, $CH_{bridgehead}$), 46.6 (s, $CH_{bridgehead}$), 68.8 (s, *C*–S), 80.4 (s, *C*H–O), 124.6 (br, *i* of BAr), 127.2 (s, CH_{dipp}), 127.2 (s, CH_{dipp}), 128.1(s, CH_{Ph}), 129.2 (s, CH_{Ph}), 130.4 (s, CH_{Ph}), 131.1 (s, CH_{Ph}), 132.1 (s, CH_{dipp}), 132.1 (s, CH_{dipp}), 133.4 (s, N–C_{Dipp}), 136.6 (br d, J_{C-F} = 244.8 Hz, Ar*C*–F), 136.7 (s, C_{PhCHO}), 138.6 (br d, J_{C-F} = 244.8 Hz, Ar*C*–F), 141.5 (s, C_{iPr}), 143.6 (s, C_{iPr}), 148.5 (br d, J_{C-F} = 241.3 Hz, Ar*C*–F), 212.9 (s, N–*C*). Signal of 3 C_{Ph} could not be detected due to overlapping. ^{19}F NMR (471 MHz, CD_2Cl_2): δ = −167.6 (t, J_{FF} = 19.2 Hz, *m* of ArC–*F*), −163.7 (t, J_{FF} = 20.4 Hz, *p* of ArC–*F*), −133.1 (br, o of ArC–*F*). ^{11}B NMR (160 MHz, CD_2Cl_2): δ = −16.7 (s, *B*Ar). ^{29}Si NMR (99 MHz, CD_2Cl_2): δ = 7.4 (s, *Si*–CH_3).

Synthesis of 2b. To a solution of **1** (150 mg, 0.13 mmol) in benzene (2.0 mL) was added acetophenone (15.7 µL, 0.13 mmol). Reaction mixture was stirred for 2 h and two phases were formed, the upper phase was removed and the lower phase washed twice with benzene (0.3 mL). Lower phase was dried under vacuum to obtained the adduct **2b** as a yellow powder as a single stereomer (88.1 mg, 53%). M.p. = 70 °C (decomposition).

^{1}H NMR (300 MHz, CD_2Cl_2): δ = 0.56 (s, 3H, Si–CH_3), 1.07 (s, 3H, Si–CH_3), 1.30 (d, $^3J_{H-H}$ = 6.6 Hz, 3H, CH_{3iPr}), 1.31 (d, $^3J_{H-H}$ = 6.6 Hz, 3H, CH_{3iPr}), 1.43 (d, $^3J_{H-H}$ = 6.6 Hz, 3H, CH_{3iPr}), 1.42 (d, $^3J_{H-H}$ = 6.6 Hz, 3H, CH_{3iPr}), 2.12 (s, 3H, $PhCOCH_3$), 2.22–1.64 (m, 5H, 3CH_2), 2.38–2.26 (m, 1H, CH_2), 2.67 (sept, $^3J_{H-H}$ = 6.6 Hz, 1H, CH_{iPr}), 3.14 (sept, $^3J_{H-H}$ = 6.6 Hz, 1H, CH_{iPr}), 3.23 (m, 1H, $CH_{bridgehead}$), 3.46 (m, 1H, $CH_{bridgehead}$), 6.31–6.17 (m, 2H, 2CH_{PhCOCH_3}), 7.68–6.89 (m, 11H, S(C_6H_5) + 3CH_{dipp} + 3CH_{PhCOCH_3}). ^{13}C NMR (75 MHz, CD_2Cl_2): δ = 1.0 (s, Si–CH_3), 2.4 (s, Si–CH_3), 24.3 (s, CH_{3iPr}), 24.5 (s, CH_{3iPr}), 25.7 (s, CH_{3iPr}), 26.3 (s, CH_{3iPr}), 28.0 (s, CH_2), 28.2 (s, CH_2), 28.3 (s, CH_{iPr}), 30.1 (s, CH_{iPr}), 42.4 (s, CH_2), 44.3 (s, $CH_{bridgehead}$), 47.5 (s, $CH_{bridgehead}$), 58.5 (s, $PhCOCH_3$), 73.5 (s, *C*–S), 83.1 (s, Ph*C*OCH_3), 127.2 (s, CH_{dipp}), 127.5 (s, CH_{dipp}), 127.6 (s, 2 C_{Ph} overlapped), 129.6 (s, C_{Ph}), 129.7 (s, C_{Ph}), 130.7 (s, C_{Ph}), 132.2 (s, CH_{dipp}), 132.3 (s, C_{Ph}), 132.5 (s, C_{Ph}), 133.7 (s, N–C_{Dipp}), 136.6 (br d, J_{C-F} = 245.2 Hz, Ar*C*–F), 138.8 (br d, J_{C-F} = 245.4 Hz, Ar*C*–F), 141.0 (s, C_{Ph}), 142.5 (s, C_{iPr}), 144.7 (s, C_{iPr}), 148.5 (br d, J_{C-F} = 241.2 Hz, Ar*C*–F), 212.2 (s, N–*C*). ^{19}F NMR (471 MHz, CD_2Cl_2): δ = −167.6 (t, J_{FF} = 19.2 Hz, *m* of ArC–*F*), −163.7 (t, J_{FF} = 20.4 Hz, *p* of ArC–*F*), −133.1 (br, o of ArC–*F*). ^{11}B NMR (160 MHz, CD_2Cl_2): δ = −16.7 (s, *B*Ar). ^{29}Si NMR (99 MHz, CD_2Cl_2): δ = 8.3 (s, *Si*–CH_3).

Synthesis of 2c. To a solution of **1** (150 mg, 0.13 mmol) in benzene (2.0 mL) was added α,α,α-trifluoroacetophenone (18.9 µL, 0.13 mmol). Reaction mixture was stirred for 4 h and two phases were formed, the upper phase was removed and the lower phase washed twice with benzene (0.3 mL). Lower phase was dried under vacuum to obtained the adduct **2c** as a pale brown powder (131.2 mg, 76%). M.p. = 71 °C (decomposition).

Major isomer (70%). ^{1}H NMR (300 MHz, CD_2Cl_2): δ = 0.68 (s, 3H, Si–CH_3), 1.24 (s, 3H, Si–CH_3), 1.49–1.27 (m, 12H, CH_{3iPr}), 2.28–1.88 (m, 5H, 3 CH_2), 2.47–2.33 (m, 1H, CH_2), 2.72 (sept, $^3J_{H-H}$ = 6.7 Hz, 1H, CH_{iPr}), 3.24 (sept, $^3J_{H-H}$ = 6.7 Hz, 1H, CH_{iPr}), 3.37 (m, 1H, $CH_{bridgehead}$), 3.83 (m, 1H, $CH_{bridgehead}$), 6.55–6.48 (m, 2H, 2 CH_{PhCOCF_3}), 7.96–6.95 (m, 11H, S(C_6H_5) + 3CH_{dipp} + 3CH_{PhCOCF_3}). ^{13}C NMR (75 MHz, CD_2Cl_2): δ = −0.5 (s, Si–CH_3), 2.8 (s, Si–CH_3), 23.9 (s, CH_{3iPr}), 24.4 (s, CH_{3iPr}), 24.9 (s, CH_{3iPr}), 25.8 (s, CH_{3iPr}), 27.4 (s, CH_2), 27.6 (s, CH_{iPr}), 27.8 (s, CH_{iPr}), 28.2 (s, CH_2), 41.2 (s, CH_2), 44.2 (s, $CH_{bridgehead}$), 47.4 (s, $CH_{bridgehead}$), 72.6 (s, *C*–S), 84.2 (q, J_{C-F} = 28.3 Hz, Ph*C*OCF_3), 123.8 (br, *i* of BAr), 127.2 (s, CH_{dipp}), 127.3 (s, CH_{dipp}), 128.3 (s, SC_{Ph}), 128.7 (s, CH_{PhCOCF_3}), 129.3 (s, CH_{PhCOCF_3}), 129.9 (s, SC_{Ph}), 130.8 (s, SC_{Ph}), 131.3 (s, SC_{Ph}), 132.1 (s, CH_{dipp}), 132.2 (s, N–C_{Dipp}), 136.3 (br d, J_{C-F} = 244.2 Hz, Ar*C*–F), 136.9 (br d, J_{C-F} = 244.5 Hz, Ar*C*–F), 138.3 (s, CH_{PhCOCF_3}), 142.7 (s, C_{iPr}), 144.3 (s, C_{iPr}), 148.1 (br d, J_{C-F} = 241.1 Hz, Ar*C*–F), 211.4 (s, N–*C*). Signal of carbon *ipso* of *Ph*COCF_3 and PhCO*C*F_3 are not visible. ^{19}F NMR (282 MHz, CD_2Cl_2): δ = −167.5 (t, J_{FF} = 19.2 Hz, *m* of ArC–*F*), −163.6 (t, J_{FF} = 20.4 Hz, *p* of ArC–*F*), −133.0 (br, o of ArC–*F*), −68.6 (br, CF_3). ^{11}B NMR (96 MHz, CD_2Cl_2): δ = −16.6 (s, *B*Ar). ^{29}Si NMR (99 MHz, CD_2Cl_2): δ = 10.5 (s, *Si*–CH_3).

Minor isomer (30%). ^{1}H NMR (300 MHz, CD_2Cl_2): δ = 0.76 (s, 3H, Si–CH_3), 0.94 (s, 3H, Si–CH_3), 1.49–1.27 (m, 12H, CH_{3iPr}), 1.72–1.63 (m, 1H, CH_2), 2.28–1.88 (m, 5H, 3CH_2), 2.68 (m, 1H, $CH_{bridgehead}$), 2.75 (sept, 1H, CH_{iPr} overlapped by CH_{iPr} of major isomer), 3.41 (m, 1H, $CH_{bridgehead}$), 3.64 (sept, $^3J_{H-H}$ = 6.7 Hz, 1H, CH_{iPr}), 6.37–6.31 (m, 2H, 2CH_{PhCOCF_3}), 7.96–6.95 (m, 11H, S(C_6H_5) + 3CH_{dipp} + 3CH_{PhCOCF_3}). ^{13}C NMR (75 MHz, CD_2Cl_2): δ =−0.3 (s, Si–CH_3), 0.5 (s, Si–CH_3), 22.8 (s, CH_{3iPr}), 23.8 (s, CH_{3iPr}), 25.9 (s, CH_{3iPr}), 26.9 (s, CH_{3iPr}), 27.6 (s, CH_2), 27.7 (s, CH_{iPr}), 27.9 (s, CH_{iPr}), 28.5 (s, CH_2), 40.2 (s, CH_2), 45.6 (s, $CH_{bridgehead}$), 47.9 (s, $CH_{bridgehead}$), 73.7 (s, *C*–S), 84.2 (Ph*C*OCF_3 overlapped with major isomer), 123.8 (br, *i* of BAr), 127.1 (s, CH_{dipp}), 127.2 (s, CH_{dipp}), 128.2 (s, SCH_{Ph}), 128.6 (s, CH_{PhCOCF_3}), 129.4 (s, CH_{PhCOCF_3}), 129.8 (s, SCH_{Ph}), 130.8 (s, SCH_{Ph} overlapped by major isomer), 131.1 (s, SC_{Ph}), 131.9 (s, CH_{PhCOCF_3}), 132.0 (s, CH_{dipp}), 132.4 (s, N–C_{Dipp}), 136.3 (br d, J_{C-F} = 244.2 Hz, Ar*C*–F), 138.3 (br d, J_{C-F} = 244.5 Hz, Ar*C*–F), 143.8 (s, C_{iPr}), 144.7 (s, C_{iPr}), 148.1 (br d, J_{C-F} = 241.1 Hz, Ar*C*–F), 210.5 (s, N–*C*). Signal of carbon *ipso* of *Ph*COCF_3 and PhCO*C*F_3 are not visible. ^{19}F NMR (282 MHz, CD_2Cl_2): δ = −167.5 (t, J_{FF} = 19.2 Hz, *m* of ArC–*F*), −163.6 (t, J_{FF} = 20.4 Hz, *p* of ArC–*F*), −133.0 (br, o of ArC–*F*), −68.1 (s, CF_3). ^{11}B NMR (96 MHz, CD_2Cl_2): δ = −16.6 (s, *B*Ar). ^{29}Si NMR (99 MHz, CD_2Cl_2): δ = 11.1 (s, *Si*–CH_3).

Synthesis of 2d. To a solution of **1** (300 mg, 0.27 mmol) in benzene (2.0 mL) was added 3-pentanone (28.5 µL, 0.27 mmol). Reaction mixture was stirred for 2 h and two phases were formed, the upper phase was removed and the lower phase washed twice with benzene (0.3 mL). Lower phase was dried under vacuum to obtained the adduct **2d** as an orange powder (263 mg, 81%). M.p. = 69 °C (decomposition).

^{1}H NMR (500 MHz, CD_2Cl_2): δ = 0.43 (s, 3H, Si–CH_3), 0.87 (s, 3H, Si–CH_3), 0.93 (t, $^3J_{H-H}$ = 7.7 Hz, 3H, CH_{3Et}), 1.15 (t, $^3J_{H-H}$ = 7.3 Hz, 3H, CH_{3Et}), 1.23 (d, $^3J_{H-H}$ = 6.7 Hz, 3H, CH_{3iPr}), 1.28 (d, $^3J_{H-H}$ = 6.6 Hz, 3H, CH_{3iPr}), 1.36 (d, $^3J_{H-H}$ = 6.6 Hz, 3H, C$H_{3\mathrm{iPr}}$), 1.37 (d, $^3J_{\mathrm{H-H}}$ = 6.7 Hz, 3H, C$H_{3\mathrm{iPr}}$), 2.18–1.75 (m, 8H, 2C$H_{2\mathrm{Et}}$ and 2CH_2), 2.29–2.20 (m, 1H, CH_2), 2.43–2.31 (m, 2H, CH_2), 2.55 (sept, $^3J_{\mathrm{H-H}}$ = 6.7 Hz, 1H, CH_{iPr}), 3.03 (sept, $^3J_{\mathrm{H-H}}$ = 6.6 Hz, 1H, CH_{iPr}), 3.12 (br, 1H, C$H_{\mathrm{bridgehead}}$), 3.37 (br, 1H, C$H_{\mathrm{bridgehead}}$), 7.61–7.37 (m, 8H, CH_{Ph}). ^{13}C NMR (126 MHz, CD_2Cl_2): δ = 0.8 (s, Si–CH$_3$), 2.5 (s, Si–CH$_3$), 8.9 (s, CH$_3$), 9.2 (s, CH$_3$), 24.2 (s, CH$_{3\mathrm{iPr}}$), 24.6 (s, CH$_{3\mathrm{iPr}}$), 25.6 (s, CH$_{3\mathrm{iPr}}$), 26.3 (s, CH$_{3\mathrm{iPr}}$), 27.4 (s, CH$_2$), 28.2 (s, CH$_{\mathrm{iPr}}$), 29.3 (s, CH$_2$), 29.7 (s, CH$_{2\mathrm{Et}}$), 30.0 (s, CH$_{\mathrm{iPr}}$), 32.8 (s, CH$_{2\mathrm{Et}}$), 41.4 (s, CH$_2$), 44.3 (s, CH$_{\mathrm{bridgehead}}$), 46.8 (s, CH$_{\mathrm{bridgehead}}$), 75.6 (s, C–S), 87.4 (s, CEt$_2$), 124.3 (br, *i* of BAr), 127.1 (s, CH$_{\mathrm{dipp}}$), 127.5 (s, CH$_{\mathrm{dipp}}$), 128.9 (s, SC_{Ph}), 129.4 (s, SC_{Ph}), 130.2 (s, SC_{Ph}), 132.1 (s, CH$_{\mathrm{dipp}}$), 132.7(s, N–C_{Dipp}), 134.6 (s, CH$_{\mathrm{Ph}}$), 136.7 (br d, $J_{\mathrm{C-F}}$ = 244.5 Hz, ArC–F), 138.6 (br d, $J_{\mathrm{C-F}}$ = 244.5 Hz, ArC–F), 144.3 (s, C_{iPr}), 142.3 (s, C_{iPr}), 148.6 (br d, $J_{\mathrm{C-F}}$ = 240.5 Hz, ArC–F), 212.9 (s, N–C). ^{19}F NMR (471 MHz, CD_2Cl_2): δ = −167.6 (t, J_{FF} = 19.2 Hz, *m* of ArC–F), −163.7 (t, J_{FF} = 20.4 Hz, *p* of ArC–F), −133.1 (br, o of ArC–F). ^{11}B NMR (160 MHz, CD_2Cl_2): δ = −16.7 (s, BAr). ^{29}Si NMR (99 MHz, CD_2Cl_2): δ = 6.4 (s, Si–CH$_3$).

Synthesis of 2e. To a solution of **1** (300.0 mg, 0.27 mmol) in benzene (2.0 mL) was added benzophenone (4.91 mg, 0.27 mmol). Reaction mixture was stirred for 2 h and precipitate was formed, solvent was removed by filtration and the solid washed twice with benzene (0.5 mL). Solid was dried under vacuum to obtained the adduct **2e** as a yellow powder (295.0 mg, 85%). Crystals were obtained from a chloroform solution at −30 °C. M.p. = 70 °C (decomposition).

^{1}H NMR (500 MHz, CD_2Cl_2): δ = 0.77 (d, $^3J_{\mathrm{H-H}}$ = 6.5 Hz, 3H, C$H_{3\mathrm{iPr}}$), 0.78 (s, 3H, Si–CH_3), 1.26 (d, $^3J_{\mathrm{H-H}}$ = 6.7 Hz, 3H, C$H_{3\mathrm{iPr}}$), 1.33 (d, $^3J_{\mathrm{H-H}}$ = 6.5 Hz, 4H, C$H_{3\mathrm{iPr}}$ + CH_2), 1.36 (s, 3H, Si–CH_3), 1.37 (d, $^3J_{\mathrm{H-H}}$ = 6.7 Hz, 3H, C$H_{3\mathrm{iPr}}$), 2.20–1.95 (m, 4H, CH_2), 2.24 (sept, $^3J_{\mathrm{H-H}}$ = 6.5 Hz, 1H, CH_{iPr}), 2.84–2.75 (m, 1H, CH_2), 2.93 (br, 1H, C$H_{\mathrm{bridgehead}}$), 3.10 (sept, $^3J_{\mathrm{H-H}}$ = 6.7 Hz, 1H, CH_{iPr}), 4.08 (br, 1H, C$H_{\mathrm{bridgehead}}$), 7.06–6.93 (m, 6H, CH_{Ph}), 7.18 (m, 1H, CH_{Ph}), 7.75–7.34 (m, 10H, CH_{Ph}). ^{13}C NMR (126 MHz, CD_2Cl_2): δ = 1.2 (s, Si–CH$_3$), 5.8 (s, Si–CH$_3$), 24.6 (s, CH$_{3\mathrm{iPr}}$), 24.9 (s, CH$_{3\mathrm{iPr}}$), 24.9 (s, CH$_{3\mathrm{iPr}}$), 25.8 (s, CH$_{3\mathrm{iPr}}$), 27.1 (s, CH$_2$), 28.6 (s, CH$_{\mathrm{iPr}}$), 28.6 (s, CH$_{\mathrm{iPr}}$), 29.2 (s, CH$_2$), 40.6 (s, CH$_2$), 45.8 (s, CH$_{\mathrm{bridgehead}}$), 47.1 (s, CH$_{\mathrm{bridgehead}}$), 76.9 (s, C–S), 89.3 (s, CPh$_2$), 124.4 (br, *i* of BAr), 127.0 (s, CH$_{\mathrm{Ph}}$), 127.2 (s, CH$_{\mathrm{dipp}}$), 127.4 (s, CH$_{\mathrm{dipp}}$), 127.6 (s, CH$_{\mathrm{Ph}}$), 128.4 (br, CH$_{\mathrm{Ph}}$), 128.8 (s, CH$_{\mathrm{Ph}}$), 128.9 (s, CH$_{\mathrm{Ph}}$), 129.6 (s, CH$_{\mathrm{Ph}}$), 129.6 (s, CH$_{\mathrm{Ph}}$), 129.7 (s, CH$_{\mathrm{Ph}}$), 131.0 (s, SC_{Ph}), 132.1 (s, CH$_{\mathrm{dipp}}$), 133.4 (s, N–C_{Dipp}), 133.5 (s, CH$_{\mathrm{Ph}}$), 136.6 (br d, $J_{\mathrm{C-F}}$ = 244.5 Hz, ArC–F), 138.7 (br d, $J_{\mathrm{C-F}}$ = 244.5 Hz, ArC–F), 140.5 (s, CPh), 141.9 (s, CPh), 142.2 (s, C_{iPr}), 143.7 (s, C_{iPr}), 148.5 (br d, $J_{\mathrm{C-F}}$ = 240.5 Hz, ArC–F), 213.2 (s, N–C). ^{19}F NMR (471 MHz, CD_2Cl_2): δ = −167.5 (t, J_{FF} = 19.2 Hz, *m* of ArC–F), −163.7 (t, J_{FF} = 20.4 Hz, *p* of ArC–F), −133.0 (br, o of ArC–F). ^{11}B NMR (160 MHz, CD_2Cl_2): δ = −16.6 (s, BAr). ^{29}Si NMR (99 MHz, CD_2Cl_2): δ = 5.5 (s, Si–CH$_3$).

Scrambling H/D reaction

In a J. Young NMR tube, to a solution of **2a** or **2c** (10 mol%) in CD_2Cl_2 was added D_1-triethylsilane (0.082 mmol, 13.1 µL) and dimethylphenylsilane (0.082 mmol, 12.6 µL) successively. Exchange reactions were monitored by ^{1}H NMR at different temperature (relaxation time D_1 = 10 s).

Hydrosilylation of acetophenone

In a J. Young NMR tube, to **2a–2e** (10 mol%) was added a solution of CD_2Cl_2 containing acetophenone (0.025 mmol), triethylsilane (0.053 mmol) and hexamethylbenzene as internal standard (0.0041 mmol). Reaction was monitored by ^{1}H NMR (relaxation time D_1 = 10 s). Conversions and selectivities were determined by ^{1}H NMR analysis of the crude samples.

Hydrosilylation of benzaldehyde

In a J. Young NMR tube, to a solution of **2a** (2.0 mol%) in CD_2Cl_2 was added benzaldehyde (0.41 mmol, 41.8 µL) and triethylsilane (0.41 mmol, 47.6 µL) successively. NMR was realized 15 minutes after and full conversion was observed.

Allylation of benzaldehyde

In a J. Young NMR tube, to a solution of **2a** (10 mol%) in CD_2Cl_2 was added benzaldehyde (0.082 mmol, 8.37 µL) and allylsilane (0.082 mmol, 13.0 µL) successively. NMR was realized 15 minutes after and full conversion was observed.

Author contributions

Conceptualization: A. B., T. K., T. M., E. M.; investigation: A. D., L. S., R. L., G. A. O. (computational); X-ray structural studies: N. S.-M.; supervision: T. M., T. K., E. M.; writing – original draft: A. D., T. K., T. M., E. M.; writing – review & editing: all authors. All authors have read and agreed to the published version of the manuscript.

Conflicts of interest

There are no conflicts to declare.

Acknowledgements

The Agence Nationale de la Recherche (ANR-16-CE07-0018-01) and the Ministère de l'Enseignement Supérieur et de la Recherche are gratefully acknowledged for Ph.D. grant to A. D. The authors would like to thanks the CNRS and the Université de Toulouse, UPS for financial support. Dr Gül Altınbaş Özpınar thanks the Philipp Schwartz Initiative of the Alexander von Humboldt Foundation for financial support. The computations were carried out at the HPC Cluster, CARL, located at the University of Oldenburg (Germany) and funded by the DFG through its Major Research Instrumentation Program (INST 184/108-1 FUGG) and the Ministry of Science and Culture (MWK) of the Lower Saxony State.

References

1 K.-C. Kim, C. A. Reed, D. W. Elliott, L. J. Mueller, F. Tham, L. Lin and J. B. Lambert, *Science*, 2002, **297**, 825–827.

2 (*a*) H. F. T. Klare and M. Oestreich, *Dalton Trans.*, 2010, **39**, 9176–9184; (*b*) A. Sekiguchi and V. Y. Lee, *Organometallic compounds of low-coordinate Si, Ge, Sn and Pb*, 2010, Wiley, Chichester; (*c*) T. Müller, Silylium ions and stabilized silylium ions in Science of Synthesis, in *Knowledge updates 2013/3*, ed. M. Oestreich and G. Thieme, Verlag KG, Stuttgart, 2013, pp. 1–42; (*d*) T. Müller, *Silylium ions in Struct. Bond*, ed. D. Scheschkewitz, 2014, vol. 155, pp. 107–162; (*e*) H. F. T. Klare, L. Albers, L. Süsse, S. Keess, T. Müller and M. Oestreich, *Chem. Rev.*, 2021, **121**, 5889–5985.

3 (*a*) M. Johannsen and K. A. Jørgensen, *J. Am. Chem. Soc.*, 1998, **120**, 7637–7638; (*b*) G. A. Olah, G. Rasul and G. K. S. Prakash, *J. Am. Chem. Soc.*, 1999, **121**, 9615–9617; (*c*) S. Duttwyler, Q.-Q. Do, A. Linden, K. K. Baldridge and J. S. Siegel, *Angew. Chem., Int. Ed.*, 2008, **47**, 1719–1722; (*d*) P. Romanato, S. Duttwyler, A. Linden, K. K. Baldridge and J. S. Siegel, *J. Am. Chem. Soc.*, 2010, **132**, 7828–7829; (*e*) P. Romanato, S. Duttwyler, A. Linden, K. K. Baldridge and J. S. Siegel, *J. Am. Chem. Soc.*, 2011, **133**, 11844–11846; (*f*) A. Schäfer, W. Saak, D. Haase and T. Müller, *Angew. Chem., Int. Ed.*, 2012, **51**, 2981–2984; (*g*) P. Ducos, V. Liautard, F. Robert and Y. Landais, *Chem. – Eur. J.*, 2015, **21**, 11573–11578; (*h*) A. Fernandes, C. Laye, S. Pramanik, D. Palmeira, O. P. Pekel, S. Massip, M. Schmidtmann, T. Müller, F. Robert and Y. Landais, *J. Am. Chem. Soc.*, 2020, **142**, 564–572; (*i*) Q. Wu, A. Roy, G. Wang, E. Irran, H. F. T. Klare and M. Oestreich, *Angew. Chem., Int. Ed.*, 2020, **59**, 10523–10526; (*j*) S. Künzler, S. Rathjen, K. Rüger, M. S. Würdemann, M. Wernke, P. Tholen, C. Girschik, M. Schmidtmann, Y. Landais and T. Müller, *Chem. – Eur. J.*, 2020, **26**, 16441–16449.

4 (*a*) B. Mathieu and L. Ghosez, *Tetrahedron Lett.*, 1997, **38**, 5497–5500; (*b*) B. Mathieu and L. Ghosez, *Tetrahedron*, 2002, **58**, 8219–8226; (*c*) J. S. Siegel, *Nat. Rev. Chem.*, 2020, **4**, 4–5; (*d*) J. C. L. Walker, H. F. T. Klare and M. Oestreich, *Nat. Rev. Chem.*, 2020, **4**, 54–62.

5 (*a*) H. F. T. Klare, K. Bergander and M. Oestreich, *Angew. Chem., Int. Ed.*, 2009, **48**, 9077–9079; (*b*) K. Müther, R. Fröhlich, C. Mück-Lichtenfeld, S. Grimme and M. Oestreich, *J. Am. Chem. Soc.*, 2011, **133**, 12442–12444; (*c*) K. Müther and M. Oestreich, *Chem. Commun.*, 2011, **47**, 334–336; (*d*) A. R. Nödling, K. Müther, V. H. G. Rohde, G. Hilt and M. Oestreich, *Organometallics*, 2014, **33**, 302–308.

6 (*a*) R. K. Schmidt, K. Müther, C. Mück-Lichtenfeld, S. Grimme and M. Oestreich, *J. Am. Chem. Soc.*, 2012, **134**, 4421–4428; (*b*) K. Müther, P. Hrobárik, V. Hrobáriková, M. Kaupp and M. Oestreich, *Chem. – Eur. J.*, 2013, **19**, 16579–16594; (*c*) K. Müther, J. Mohr and M. Oestreich, *Organometallics*, 2013, **32**, 6643–6646.

7 K. Müther and M. Oestreich, *Chem. Commun.*, 2011, **47**, 334–336.

8 (*a*) V. J. Scott, Ç.-Ç. Remle and O. V. Ozerov, *J. Am. Chem. Soc.*, 2005, **127**, 2852–2853; (*b*) R. Panisch, M. Bolte and T. Müller, *J. Am. Chem. Soc.*, 2006, **128**, 9676–9682; (*c*) C. Douvris and O. V. Ozerov, *Science*, 2008, **321**, 1188–1190; (*d*) C. Douvris, C. M. Nagaraja, C. H. Chen, B. M. Foxman and O. V. Ozerov, *J. Am. Chem. Soc.*, 2010, **132**, 4946–4953; (*e*) N. Lühmann, R. Panisch and T. Müller, *Appl. Organomet. Chem.*, 2010, **24**, 533–537; (*f*) N. Lühmann, H. Hirao, S. Shaik and T. Müller, *Organometallics*, 2011, **30**, 4087–4096; (*g*) O. Allemann, S. Duttwyler, K. K. Baldridge and J. S. Siegel, *Science*, 2011, **332**, 574–577; (*h*) T. Stahl, H. F. T. Klare and M. Oestreich, *ACS Catal.*, 2013, **3**, 1578–1587; (*i*) N. Kordts, C. Borner, R. Panisch, W. Saak and T. Müller, *Organometallics*, 2014, **33**, 1492–1498; (*j*) N. Kordts, S. Künzler, S. Rathjen, T. Sieling, H. Groβekappenberg, M. Schmidtmann and T. Müller, *Chem. – Eur. J.*, 2017, **23**, 10068–10079; see also: I. Mallov, A. J. Ruddy, H. Zhu, S. Grimme and D. W. Stephan, *Chem. – Eur. J.*, 2017, **23**, 17692–17696. for a P/[Si+]-frustrated Lewis pair.

9 Electrodeficient phosphorus species such as phosphenium or phosphonium should also be mentioned as efficient catalyst to promote hydrodefluorination see: (*a*) C. B. Caputo, L. J. Hounjet, R. Dobrovetsky and D. W. Stephan, *Science*, 2013, **341**, 1374–1377; (*b*) J. M. Bayne and D. W. Stephan, *Chem. Soc. Rev.*, 2016, **45**, 765–774; (*c*) J. Zhu, M. Pérez, C. B. Caputo and D. W. Stephan, *Angew. Chem., Int. Ed.*, 2016, **55**, 1417–1421; (*d*) J. Zhu, M. Pérez and D. W. Stephan, *Angew. Chem., Int. Ed.*, 2016, **55**, 8448–8451; (*e*) J. M. Bayne and D. W. Stephan, *Chem. – Eur. J.*, 2019, **25**, 9350–9357.

10 (*a*) A. Dajnak, E. Maerten, N. Saffon-Merceron, A. Baceiredo and T. Kato, *Organometallics*, 2020, **39**, 3403–3412; (*b*) A. Dajnak, G. A. Özpınar, R. Lenk, N. Saffon-Merceron, A. Baceiredo, T. Kato, T. Müller and E. Maerten, *Dalton Trans.*, 2022, **51**, 1407–1414.

11 For other sulfide-stabilized silylium ions see: (*a*) V. H. G. Rohde, P. Pommerening, H. F. T. Klare and M. Oestreich, *Organometallics*, 2014, **33**, 3618–3628; (*b*) V. H. G. Rohde, M. F. Müller and M. Oestreich, *Organometallics*, 2015, **34**, 3358–3373; (*c*) A. Simonneau, T. Biberger and M. Oestreich, *Organometallics*, 2015, **34**, 3927–3829; (*d*) P. Shaykhutdinova and M. Oestreich, *Organometallics*, 2016, **35**, 2768–2771; (*e*) P. Shaykhutdinova, S. Kemper and M. Oestreich, *Eur. J. Org. Chem.*, 2018, 2896–2901; (*f*) P. Shaykhutdinova and M. Oestreich, *Org. Lett.*, 2018, **20**, 7029–7033; (*g*) P. Shaykhutdinova and M. Oestreich, *Synthesis*, 2019, 2221–2229; (*h*) A. Falk and J. O. Bauer, *Inorg. Chem.*, 2022, **61**(39), 15576–15588.

12 (*a*) T. Ochiai, T. Szilvasi and S. Inoue, *Molecules*, 2016, **21**, 1155; (*b*) S. Courtenay, C. M. Ong and D. W. Stephan, *Organometallics*, 2003, **22**(4), 818–825.

13 V. Fasano, J. E. Radcliffe, L. D. Curless and M. J. Ingleson, *Chem. – Eur. J.*, 2017, **23**, 187–193.

14 (*a*) M. Kira, T. Hino and H. Sakurai, *Chem. Lett.*, 1992, **21**, 555–558; (*b*) D. J. Parks, J. M. Blackwell and W. E. Piers, *J. Org. Chem.*, 2000, **65**, 3090–3098.

15 Reaction with catalyst **2b** was also performed at 0 °C to favor selectivity toward the silylated alcohol **A** without success (51% conv. after 24 h, 39% **A**, 8% **B**).